arXiv:1703.02059v1 [stat.ML] 6 Mar 2017

CHESHIRE: An Online Algorithm for Activity Maximization in Social Networks

Ali Zarezade*[1], Abir De*[2], Hamid R. Rabiee[1], and Manuel Gomez-Rodriguez[3]

[1]Sharif University, zarezade@ce.sharif.edu
[2]IIT Kharagpur, abir.de@cse.iitkgp.ernet.in
[3]Max Planck Institute for Software Systems, manuelgr@mpi-sws.org

Abstract

User engagement in social networks depends critically on the number of online *actions* their users take in the network. Can we design an algorithm that finds when to incentivize users to take actions to maximize the overall activity in a social network? In this paper, we model the number of online actions over time using multidimensional Hawkes processes, derive an alternate representation of these processes based on stochastic differential equations (SDEs) with jumps and, exploiting this alternate representation, address the above question from the perspective of stochastic optimal control of SDEs with jumps. We find that the optimal level of incentivized actions depends linearly on the current level of overall actions. Moreover, the coefficients of this linear relationship can be found by solving a matrix Riccati differential equation, which can be solved efficiently, and a first order differential equation, which has a closed form solution. As a result, we are able to design an efficient online algorithm, CHESHIRE, to sample the optimal times of the users' incentivized actions. Experiments on both synthetic and real data gathered from Twitter show that our algorithm is able to consistently maximize the number of online actions more effectively than the state of the art.

1 Introduction

People are constantly performing a wide variety of online actions in a growing number of online platforms such as social networking sites, question answering (Q&A) sites or wikis. In most of these platforms, these actions can be *exogenous*, taken by users at their own initiative, or *endogenous* actions, taken by users as a *response* to previous actions by other users. For example, in social networking sites, users post small pieces of information, which can then trigger likes, shares or replies by other users; in Q&A sites, users can ask questions, which are then answered and curated by other users; or, in wikis, editors write content, which is later reviewed and refined by other editors in a collaborative fashion. In this context, a natural question emerges: how much should we incentivize a small number of users to take more initiatives to drive the overall number of actions to a certain level (*e.g.*, at least twice actions per day per user)?

The "activity shaping" problem was first studied by Farajtabar et al. [8], who derived a time dependent linear relation between the *intensity* of exogenous actions and the overall intensity of actions in a social network under a model of actions based on multivariate Hawkes processes and, exploiting this connection, developed a convex optimization framework for activity shaping. One of the main shortcomings of their framework is that it provides deterministic exogenous intensities that do not adapt to changes in the users' intensities and, as a consequence, it is less effective than our proposed algorithm, as shown in Section 5.

*Authors contributed equally. This work was done during Ali Zarezade's and Abir De's internships at Max Planck Institute for Software Systems.

More recently, Farajtabar et al. [10] developed a heuristic method that splits the time window of interest into stages and adapts to changes in the users' intensities at the beginning of each stage. However, their method is suboptimal, it does not have *provable* guarantees, and it achieves lower performance than our method.

In this paper, we design a novel online algorithm for the "activity maximization" problem in social networks, one of the most important instances of the activity shaping problem, in which the goal is to maximize the number of actions in the network.[1] More in detail, we represent users' actions using the framework of temporal point processes, which characterizes the continuous time interval between actions using conditional intensity functions [1], and model endogenous and exogenous actions using multidimensional Hawkes processes [15]. Then, we derive an alternate representation of multidimensional Hawkes processes using SDEs with jumps and, exploiting this alternate representation, cast the activity maximization problem as a novel optimal control problem for SDEs with jumps. Our problem formulation differs from the traditional control literature [14] in two key technical aspects, which have not been considered until very recently [31]:

I. The control signal, used to sample the times of incentivized actions, is a multidimensional conditional intensity while previous work considered the control signal to be a time-varying real vector.

II. The users' intensities are stochastic Markov processes and thus the dynamics are doubly stochastic. In contrast, previous work considered deterministic (typically constant) intensities.

Moreover, we find that the optimal level of incentivized actions depends linearly on the current level of overall actions. Moreover, the coefficients of this linear relationship can be found by solving a matrix Riccati differential equation, which can be solved using many well-known efficient numerical solvers [12], and a first order differential equation, which has closed form solution. This allows for an efficient and relatively simple online procedure to sample the optimal times of the users' incentivized actions, which can be implemented in a few lines of code (refer to Algorithm 1). Finally, we perform experiments on both synthetic and real data gathered from Twitter and show that our method is able to consistently maximize the number of actions more effectively than the state of the art [8, 10].

1.1 Further related work

In addition to the paucity of work on the activity shaping problem [8, 10], discussed previously, our work also relates to previous work on stochastic optimal control, the influence maximization problem, and temporal point processes.

In the traditional control literature [14], two key aspects of our problem formulation—intensities as control signals and stochastic intensities—have been large understudied. Only very recently, Zarezade et al. [31] and Wang et al. [30] have considered these aspects, however, our approach differs in several ways: The work by Zarezade et al. is more closely related to ours, however, they solve a different problem, the when-to-post problem [26], where one aims to optimize a social network user's broadcasting strategy to capture the greatest attention from the followers. Such problem is significantly less challenging than activity maximization—it only considers 1-hop information propagation—and, as a consequence, their resulting sampling algorithm is very different to ours. The work by Wang et al. focuses on two different problems, the when-to-post problem and opinion control, their strategy is open-loop and their control policy depends on the expectation of the uncontrolled dynamics, which needs to be calculated approximately by a time consuming sampling process. In contrast, our framework is closed-loop, our control policy only depends on the current state of the dynamics and the feedback coefficients only need to be calculated once off-line.

The influence maximization problem [4, 6, 17, 25] aims to find a set of nodes in a social network whose initial adoption of a certain idea or product can trigger the largest expected number of follow-ups. However, previous work on the influence maximization problem differs from our work in two main aspects. First, in influence maximization, the state of each user is often assumed to be binary, either adopting a product or not. However, such assumption does not capture the recurrent nature of product usage, where the frequency of the usage matters. Second, while influence maximization methods identify a set of users to provide incentives,

[1] Our methodology can be easily extended to online platforms without an explicit underlying network between users. However, for ease of exposition, we focus on social networking sites.

they do not typically provide a quantitative prescription on how much incentive should be provided to each user.

Temporal point processes has been increasingly used for representation and modeling in a wide range of applications in social and information systems, *e.g.*, information propagation [13, 6, 32], opinion dynamics [5], product competition [29], information reliability [28], or human learning [22]. However, in such context, there is still a paucity of algorithms based on stochastic optimal control of temporal point processes [31, 30].

2 Preliminaries

In this section, we first revise the framework of temporal point processes [1] and then describe how to use such framework to model endogenous and exogenous actions in social networks [7].

2.1 Temporal point processes

A univariate temporal point process is a stochastic process whose realization consists of a sequence of discrete events localized in time, $\mathcal{H} = \{t_i \in \mathbb{R}_+ \,|\, i \in \mathbb{N}_+,\, t_i < t_{i+1}\}$. A univariate temporal point process can be equivalently represented by a counting process $N(t)$, which counts the number of events before time t, *i.e.*,

$$N(t) = \sum_{t_i \in \mathcal{H}} u(t - t_i),$$

where $u(t) = 1$ if $t \geq 0$ and $u(t) = 0$ otherwise. Then, we can characterize the counting process using the conditional intensity function $\lambda^*(t)$, which is the conditional probability of observing an event in an infinitesimal window $[t, t + dt)$ given the history of event times up to time t, $\mathcal{H}(t) = \{t_i \in \mathcal{H} \,|\, t_i < t\}$, *i.e.*,

$$\lambda^*(t)\, dt = \mathbb{P}\left\{\text{event in } [t, t + dt) \,|\, \mathcal{H}(t)\right\} = \mathbb{E}[dN(t) \,|\, \mathcal{H}(t)],$$

where $dN(t) := N(t+dt) - N(t) \in \{0, 1\}$, the sign * means that the intensity may depend on the history $\mathcal{H}(t)$, and the functional form for the intensity is often designed to capture the phenomena of interest. Moreover, given a function $f(t)$, it will be useful to define the convolution with respect to $dN(t)$ as

$$f(t) \star dN(t) := \int_0^t f(t - s) dN(s) = \sum_{t_i \in \mathcal{H}(t)} f(t - t_i).$$

One can readily extend the above definitions to multivariate (or multidimensional) temporal point processes, which have been recently used to represent many different types of event data produced in social networks, such as the times of tweets [16], retweets [32] or links [9]. More specifically, a realization of an m-dimensional temporal point process consists of m sequences of discrete events localized in time, $\mathcal{H} = \cup_{u \in [m]} \mathcal{H}_u$, where $\mathcal{H}_u = \{t_i | t_i \in \mathbb{R}_+ \,|\, i \in \mathbb{N}_+,\, t_i < t_{i+1}\}$, and it can be represented by an m-dimensional counting process $\mathbf{N}(t)$, where $N_u(t)$ counts the number of events in the u-th sequence before time t. Similarly, such counting process can be characterized by m intensity functions, *i.e.*,

$$\boldsymbol{\lambda}^*(t)dt = \mathbb{E}[d\boldsymbol{N}(t)|\mathcal{H}(t)],$$

where $\boldsymbol{\lambda}^*(t) = (\lambda_1^*(t), \ldots, \lambda_m^*(t))$ and $\mathcal{H}(t) = \{t_i \in \mathcal{H} | t_i < t\}$, and, given a function $f(t)$, one can define the convolution with respect to $d\boldsymbol{N}(t)$ as

$$\int_0^t f(t - s) d\boldsymbol{N}(s) = \Big(\sum_{t_i \in \mathcal{H}_u(t)} f(t - t_i) \Big)_{u \in [m]}.$$

Next, we use the above background to revisit how to jointly model endogenous and exogenous actions in social networks [7] and then derive an alternate model representation based on SDEs with jumps, which will be useful to design our stochastic optimal control algorithm.

2.2 Modeling endogenous and exogenous actions in social networks

Given a directed network $\mathcal{G} = (\mathcal{V}, \mathcal{E})$ with $|\mathcal{V}| = n$ users, we model both endogenous and exogenous actions taken by all the users using an m-dimensional Hawkes process $\boldsymbol{N}(t)$, where $N_u(t)$ counts the number of actions taken by user u before time t. More specifically, the intensities of this process are given by [7, 15]:

$$\boldsymbol{\lambda}^*(t) = \boldsymbol{\mu}_0 + \boldsymbol{A} \int_0^t \kappa(t-s)\, d\boldsymbol{N}(s), \tag{1}$$

where the first term models exogenous actions—actions users take at their own initiative—and the second term model endogenous actions—actions users take as response to the actions taken by their neighbors within the network. Here, we parametrize the strength of *influence* between users using a sparse nonnegative *influence matrix* $\boldsymbol{A} = (a_{uv}) \in \mathbb{R}_+^{m \times m}$, where a_{uv} means user u's actions directly triggers *follow-ups* from user v, and $\kappa(t) = e^{-\omega t}\, u(t)$ is an exponential kernel modeling the decay of influence over time. Note that the second term makes the intensities dependent on the history and thus a stochastic process by itself. In the remainder of the paper, we drop the sign * from the intensities for the notational convenience.

The following alternative representation of the above process will be useful to design our stochastic optimal control algorithm for the activity maximization (proven in Appendix A):

Proposition 1 *Let $\boldsymbol{N}(t)$ be an m-dimensional counting process with an associated intensity $\boldsymbol{\lambda}(t)$ given by Eq. 1. Then, the tuple $(\boldsymbol{N}(t), \boldsymbol{\lambda}(t))$ is a doubly stochastic Markov process, whose dynamics can be defined by the following jump SDEs:*

$$d\boldsymbol{\lambda}(t) = [w\boldsymbol{\mu}_0 - w\boldsymbol{\lambda}(t)]\, dt + \boldsymbol{A}\, d\boldsymbol{N}(t), \tag{2}$$

with the initial condition $\boldsymbol{\lambda}(0) = \boldsymbol{\lambda}_0$.

3 Problem Formulation

In this section, we first describe a mechanism to steer endogenous actions in social networks and then formally state the online activity maximization problem for such mechanism.

3.1 Steering endogenous actions

We steer endogenous actions (or events) in the counting process $\boldsymbol{N}(t)$ by introducing a counting process $\boldsymbol{M}(t)$, with control intensities $\boldsymbol{u}(t)$, which triggers additional follow-ups. More specifically, this counting process modulates the corresponding intensities $\boldsymbol{\lambda}(t)$ as follows:

$$\boldsymbol{\lambda}^*(t) = \underbrace{\boldsymbol{\mu}_0 + \boldsymbol{A} \int_0^t \kappa(t-s)\, d\boldsymbol{N}(s)}_{\text{Organic actions}} + \underbrace{\boldsymbol{A} \int_0^t \kappa(t-s)\, d\boldsymbol{M}(s)}_{\text{Incentivized actions}}, \tag{3}$$

where we assume the strength of influence $\boldsymbol{A}$ between users is the same both for the organic and incentivized actions, as previous work [7, 10]. Then, it is easy to derive the following alternative representation, similarly as in Proposition 1, which we will use in our stochastic optimal control algorithm:

Proposition 2 *Let $\boldsymbol{N}(t)$ be a multidimensional counting process with associated intensities $\boldsymbol{\lambda}(t)$, given by Eq. 3, and $\boldsymbol{M}(t)$ be a controllable counting process with an associated intensity $\boldsymbol{u}(t)$. Then, the system dynamics can be defined by the following jump SDEs:*

$$d\boldsymbol{\lambda}(t) = [w\boldsymbol{\mu}_0 - w\boldsymbol{\lambda}(t)]\, dt + \boldsymbol{A}\, d\boldsymbol{N}(t) + \boldsymbol{A}\, d\boldsymbol{M}(t) \tag{4}$$

with the initial condition $\boldsymbol{\lambda}^*(0) = \boldsymbol{\lambda}_0$.

3.2 The (online) activity maximization problem

Given a directed network $\mathcal{G} = (\mathcal{V}, \mathcal{E})$ with $|\mathcal{V}| = n$ users, our goal is to find the optimal control intensities $\boldsymbol{u}(t)$ that minimize the expected value of a particular loss function $\ell(\boldsymbol{\lambda}(t), \boldsymbol{u}(t))$ of the users's organic and control intensities over a time window $(t_0, t_f]$, *i.e.*,

$$\begin{aligned} \underset{\boldsymbol{u}(t_0,t_f]}{\text{minimize}} \quad & \mathbb{E}_{(\boldsymbol{N},\boldsymbol{M})(t_0,t_f]} \left[\phi(\boldsymbol{\lambda}(t_f)) + \int_{t_0}^{t_f} \ell(\boldsymbol{\lambda}(t), \boldsymbol{u}(t))\, dt \right] \\ \text{subject to} \quad & u_i(t) \geq 0,\ \forall t \in (t_0, t_f],\ i = 1, \ldots, n \end{aligned} \tag{5}$$

where $\boldsymbol{u}(t_0, t_f]$ denotes the control intensity functions from t_0 to t_f, the dynamics of $\boldsymbol{N}(t)$ are given by Eq. 4, and the expectation is taken over all possible realizations of the two counting process $\boldsymbol{N}(t)$ and $\boldsymbol{M}(t)$ during interval $(t_0, t_f]$. Here, by considering a loss that is nonincreasing with respect to the organic intensities $\boldsymbol{\lambda}(t)$, we will penalize low organic intensities, and, by considering a loss that is nondecreasing with respect to the control intensities $\boldsymbol{u}(t)$, we will limit the number of posts we steer. Finally, note that the optimal intensities $\boldsymbol{u}(t)$ at time t may depend on the organic intensities $\boldsymbol{\lambda}(t)$ and thus the associated counting process $\boldsymbol{M}(t)$ may be doubly stochastic.

4 Stochastic Optimal Control Algorithm

In this section, we tackle the activity maximization problem defined by Eq. 5 from the perspective of stochastic optimal control of jump SDEs [14]. More specifically, we first define a novel optimal cost-to-go function that accounts for the above unique aspects of our problem, show that the Bellman's principle of optimality [2] still follows, and finally derive and solve the Hamilton-Jacobi-Bellman (HJB) equation to find the optimal control intensity.

Definition 3 *The optimal cost-to-go is defined as the minimum of the expected value of the cost of going from the state with intensity $\boldsymbol{\lambda}(t)$ at time t to the final state at time t_f.*

$$J(\boldsymbol{\lambda}(t), t) = \min_{\boldsymbol{u}(t,t_f]} \mathbb{E}_{(\boldsymbol{N},\boldsymbol{M})(t,t_f]} \left[\phi(\boldsymbol{\lambda}(t_f)) + \int_{t}^{t_f} \ell(\boldsymbol{\lambda}(s), \boldsymbol{u}(s))\, ds \right], \tag{6}$$

where the expectation is taken over all trajectories of the counting processes $\boldsymbol{N}$ and $\boldsymbol{M}$ in the $(t, t_f]$ interval, given the initial values of $\boldsymbol{\lambda}(t)$ and $\boldsymbol{u}(t)$.

To find the optimal control $u(t, t_f]$ and cost-to-go J, we break the problem into smaller subproblems, using Bellman's principle of optimality (proven in the Appendix B):

Theorem 4 (Bellman's Principle of Optimality) *The optimal cost-to-go function defined by Eq. 6 satisfies the following recursive equation:*

$$J(\boldsymbol{\lambda}(t), t) = \min_{\boldsymbol{u}(t,t+dt]} \left\{ \mathbb{E}_{(\boldsymbol{N},\boldsymbol{M})(t,t+dt]} \left[J(\boldsymbol{\lambda}(t + dt), t + dt) \right] + \ell(\boldsymbol{\lambda}(t), \boldsymbol{u}(t))\, dt \right\} \tag{7}$$

where the expectation is taken over all realizations of the counting processes $\boldsymbol{N}(t)$ and $\boldsymbol{M}(t)$ in the infinitesimal interval $(t, t + dt]$.

Next, we use the Bellman's principle of optimality to derive a partial differential equation on J, often called HJB equation. To do so, we first assume J is continuous and then rewrite Eq. 7 as

$$\begin{aligned} J(\boldsymbol{\lambda}(t), t) &= \min_{\boldsymbol{u}(t,t+dt]} \left\{ \mathbb{E}_{(\boldsymbol{N},\boldsymbol{M})(t,t+dt]} \left[J(\boldsymbol{\lambda}(t), t) + dJ(\boldsymbol{\lambda}(t), t) \right] + \ell(\boldsymbol{\lambda}(t), \boldsymbol{u}(t))\, dt \right\} \\ 0 &= \min_{\boldsymbol{u}(t,t+dt]} \left\{ \mathbb{E}_{(\boldsymbol{N},\boldsymbol{M})(t,t+dt]} \left[dJ(\boldsymbol{\lambda}(t), t) \right] + \ell(\boldsymbol{\lambda}(t), \boldsymbol{u}(t))\, dt \right\} \end{aligned} \tag{8}$$

Then, we differentiate J with respect to time t and $\lambda(t)$ according to Ito's calculus [14] by the following Lemma (proven in the Appendix C):

Theorem 5 *The differential of the cost-to-go function $J(\boldsymbol{\lambda}(t), t)$ given by Eq. 6 is given by:*

$$dJ(\boldsymbol{\lambda}(t),t) = J_t(\boldsymbol{\lambda}(t),t)\,dt + [w\boldsymbol{\mu}_0 - w\boldsymbol{\lambda}(t)]^T \nabla_{\boldsymbol{\lambda}} J(\boldsymbol{\lambda}(t),t)\,dt + \sum_{i=1}^{n} \left[J(\boldsymbol{\lambda}(t)+\boldsymbol{a}_i,t) - J(\boldsymbol{\lambda}(t),t)\right]\left[dN_i(t) + dM_i(t)\right]$$

where $\boldsymbol{a}_i$ is the i'th column of $\boldsymbol{A}$, J_t is derivative of J with respect to t and $\nabla_{\boldsymbol{\lambda}}$ is the gradient of J with respect to $\boldsymbol{\lambda}(t)$.

Next, if we plug the above equation in Eq. 8, then use $\mathbb{E}[N_i(t)] = \lambda_i(t)\,dt$, and $\mathbb{E}[M_i(t)] = u_i(t)\,dt$, the HJB equation follows:

$$0 = J_t(\boldsymbol{\lambda}(t),t) + [w\boldsymbol{\mu}_0 - w\boldsymbol{\lambda}(t)]^T \nabla_{\boldsymbol{\lambda}} J(\boldsymbol{\lambda}(t),t) + \boldsymbol{\lambda}^T(t)\,\Delta_A J + \min_{\boldsymbol{u}(t)} \ell(\boldsymbol{\lambda}(t),\boldsymbol{u}(t)) + \boldsymbol{u}^T(t)\,\Delta_A J \tag{9}$$

where $\Delta_A J$ denotes a vector whose i'th element is given by $(\Delta_A J)_i = J(\boldsymbol{\lambda}(t)+\boldsymbol{a}_i,t) - J(\boldsymbol{\lambda}(t),t)$.

To solve the above equation, we need to define the loss and penalty functions, ℓ and ϕ. Following the literature on stochastic optimal control [2, 14], we consider the following quadratic forms, which will turn out to be a tractable choice:

$$\begin{aligned} \ell(\boldsymbol{\lambda}(t),\boldsymbol{u}(t)) &= -\frac{1}{2}\boldsymbol{\lambda}^T(t)\,\boldsymbol{Q}\,\boldsymbol{\lambda}(t) + \frac{1}{2}\boldsymbol{u}^T(t)\,\boldsymbol{S}\,\boldsymbol{u}(t) \\ \phi(\boldsymbol{\lambda}(t_f)) &= -\frac{1}{2}\boldsymbol{\lambda}^T(t_f)\,\boldsymbol{F}\,\boldsymbol{\lambda}(t_f) \end{aligned} \tag{10}$$

where $\boldsymbol{Q}$, $\boldsymbol{F}$ and $\boldsymbol{S}$ are given symmetric matrices[2] with $q_{ij} \geq 0$, $f_{ij} \geq 0$ and $s_{ij} \geq 0$ for all $i, j \in [n]$. These matrices allow us to trade-off the number of non incentivized actions, both over time and at time t_f, and the number of incentivized actions. Under these definitions, we can find the relationship between the optimal intensity and the optimal cost by solving the minimization in the HJB Eq. 9.

$$\begin{aligned} \underset{\boldsymbol{u}(t)}{\text{minimize}} \quad & \boldsymbol{u}^T(t)\,\Delta_A J + \frac{1}{2}\boldsymbol{u}^T(t)\,\boldsymbol{S}\,\boldsymbol{u}(t) \\ \text{subject to} \quad & u_i(t) \geq 0,\ i = 1,\ldots,n \end{aligned}$$

By taking the differentiation with respect to $\boldsymbol{u}(t)$, the solution of the unconstrained minimization is given by:

$$\boldsymbol{u}^*(t) = -\boldsymbol{S}^{-1}\Delta_A J, \tag{11}$$

which is the same to the solution of the constraint problem, since $(\Delta_A J)_i \leq 0$, as proved in the Appendix D, and $s_{ij} \geq 0$ by definition.

Then, we substitute Eq. 11 into Eq. 9 and find that the optimal cost J needs to satisfy the following partial differential equation:

$$0 = J_t(\boldsymbol{\lambda}(t),t) + [w\boldsymbol{\mu}_0 - w\boldsymbol{\lambda}(t)]^T \nabla_{\boldsymbol{\lambda}} J(\boldsymbol{\lambda}(t),t) + \boldsymbol{\lambda}^T(t)\,\Delta_A J - \frac{1}{2}\boldsymbol{\lambda}^T(t)\,\boldsymbol{Q}\,\boldsymbol{\lambda}(t) - \frac{1}{2}\Delta_A J^T \boldsymbol{S}^{-1}\Delta_A J \tag{12}$$

with $J(\boldsymbol{\lambda}(t_f), t_f) = \phi(\boldsymbol{\lambda}(t_f))$ as the terminal condition. The following lemma provides us with a solution to the above equation (proven in Appendix E):

Lemma 6 *Any solution to the nonlinear differential equation given by Eq. 12 can be approximated as desired by the following quadratic form:*

$$J(\boldsymbol{\lambda}(t),t) = f(t) + \boldsymbol{g}(t)^T\boldsymbol{\lambda}(t) + \frac{1}{2}\boldsymbol{\lambda}(t)^T\boldsymbol{H}(t)\boldsymbol{\lambda}(t).$$

where $\boldsymbol{g}(t)$ and $\boldsymbol{H}(t)$ can be found by solving the following differential equations:

$$\begin{aligned} \dot{\boldsymbol{H}}(t) &= (\omega\boldsymbol{I} - \boldsymbol{A})^T\boldsymbol{H}(t) + \boldsymbol{H}(t)(\omega\boldsymbol{I} - \boldsymbol{A}) + \boldsymbol{H}(t)\boldsymbol{A}\boldsymbol{S}^{-1}\boldsymbol{A}^T\boldsymbol{H}(t) + \boldsymbol{Q} \\ \dot{\boldsymbol{g}}(t) &= [\omega\boldsymbol{I} - \boldsymbol{A}^T + \boldsymbol{H}(t)\boldsymbol{A}\boldsymbol{S}^{-1}\boldsymbol{A}^T]\boldsymbol{g}(t) - \omega\boldsymbol{H}(t)\boldsymbol{\mu}_0 + \frac{1}{2}\left[\boldsymbol{H}(t)\boldsymbol{A}\boldsymbol{S}^{-1} - \boldsymbol{I}\right]\mathrm{diag}(\boldsymbol{A}^T\boldsymbol{H}(t)\boldsymbol{A}) \end{aligned}$$

Algorithm 1: CHESHIRE: it returns user i and time τ for the next incentivized action.

1: **Initialization:**
2: Compute $\boldsymbol{H}(t)$ and $\mathbf{g}(t)$;
3: $\mathbf{u}(t) \leftarrow -\boldsymbol{S}^{-1}\big[\boldsymbol{A}^T(\boldsymbol{g}(t) + \boldsymbol{H}(t)\boldsymbol{\mu}_0) + \frac{1}{2}\operatorname{diag}(\boldsymbol{A}^T\boldsymbol{H}(t)\boldsymbol{A})\big]$;
4: **General subroutine:**
5: $(i, \tau) \leftarrow \mathit{Sample}(\mathbf{u}(t))$;
6: $(j, s) \leftarrow \mathit{NextAction}(\,)$;
7: **while** $s < \tau$ **do**
8: $\quad \boldsymbol{\lambda}_N(t) \leftarrow \boldsymbol{A}\mathbf{e}_j\kappa(t - s)$;
9: $\quad \mathbf{u}_N(t) \leftarrow -\boldsymbol{S}^{-1}\boldsymbol{A}^T\boldsymbol{H}(t)\boldsymbol{\lambda}_N(t)$;
10: $\quad (k, r) \leftarrow \mathit{Sample}(\mathbf{u}_N(t))$;
11: $\quad$ **if** $r < \tau$ **then**
12: $\quad\quad \tau \leftarrow r$;
13: $\quad\quad i \leftarrow k$;
14: $\quad \mathbf{u}(t) \leftarrow \mathbf{u}(t) + \mathbf{u}_N(t)$;
15: $\quad (j, s) \leftarrow \mathit{NextAction}(\,)$;
16: $\boldsymbol{\lambda}_M(t) \leftarrow \boldsymbol{A}\mathbf{e}_i\kappa(t - \tau)$;
17: $\mathbf{u}_M(t) \leftarrow -\boldsymbol{S}^{-1}\boldsymbol{A}^T\boldsymbol{H}(t)\boldsymbol{\lambda}_M(t)$;
18: $\mathbf{u}(t) \leftarrow \mathbf{u}(t) + \mathbf{u}_M(t)$;
19: **return** (i, τ)

In the above lemma, note that the first differential equation is a matrix Riccati differential equation, which can be solved using many well-known efficient numerical solvers [12], and the second one is a first order differential equation which has closed form solution. Both equations are solved backward in time with final conditions $\boldsymbol{g}(t_f) = \mathbf{0}$ and $\boldsymbol{H}(t_f) = -\boldsymbol{F}$.

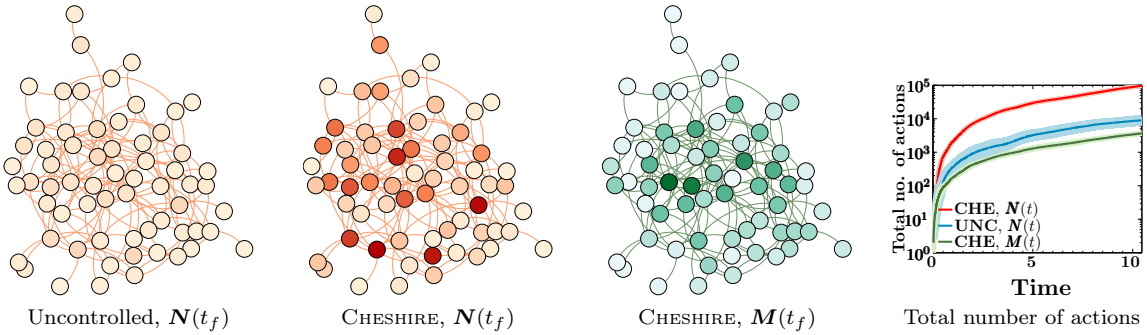
Finally, given the above cost-to-go function, the optimal intensity is given by the following theorem, *i.e.*,

Theorem 7 *The optimal intensity for the activity maximization problem defined by Eq. 5 with quadratic loss and penalty function is given by:*

$$\boldsymbol{u}^*(t) = -\boldsymbol{S}^{-1}\big[\boldsymbol{A}^T\boldsymbol{g}(t) + \boldsymbol{A}^T\boldsymbol{H}(t)\boldsymbol{\lambda}(t) + \frac{1}{2}\operatorname{diag}(\boldsymbol{A}^T\boldsymbol{H}(t)\boldsymbol{A})\big] \tag{13}$$

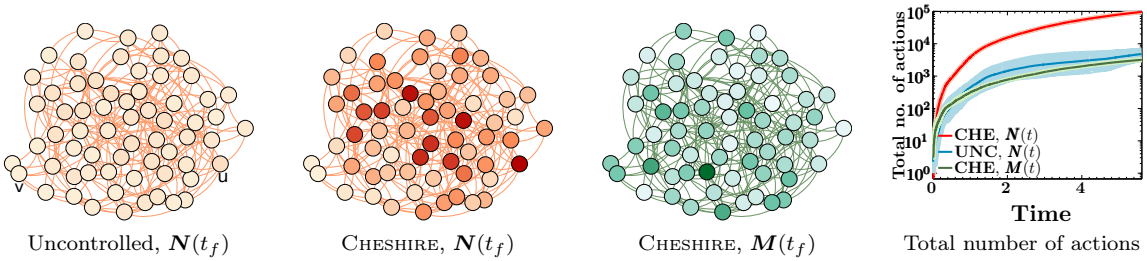
This optimal intensity is linear in $\boldsymbol{\lambda}(t)$ and the coefficients $\boldsymbol{g}(t)$ and $\boldsymbol{H}(t)$ can be found off-line. Hence, it allows for a very efficient procedure to sample the times of the users' incentivized actions, which takes inspiration from the algorithm REDQUEEN [31].. The key idea is as follows.

At any given time t, we can view the multidimensional control signal $\boldsymbol{u}(t)$ as a superposition of inhomogeneous multidimensional poisson processes, one per non incentivized action, which start when the actions take place. Algorithm 1 summarizes our method, which we name CHESHIRE [3]. Within the algorithm, *NextAction*() returns the time of the next (non incentivized) action in the network as well as the identify of the user who takes the action, once the action happens, $\boldsymbol{e}_j$ is an indicator vector where the entry corresponding to user j is 1, and *Sample*($\boldsymbol{u}(t)$) samples from a multidimensional inhomogeneous poisson process with intensity $\boldsymbol{u}(t)$ and it returns both the sampled time and dimension. To sample from a multidimensional inhomogeneous poisson process, there exist multiple methods *e.g.*, refer to Lewis et al. [21]. Finally, note that one can precompute most of the quantities the algorithm needs, *i.e.*, lines 2-3, $\boldsymbol{A}\boldsymbol{e}_j$ in line 8, and $\boldsymbol{S}^{-1}\boldsymbol{A}^T\boldsymbol{H}(t)$ in line 9. Given these precomputations, the algorithm only needs to perform $O(n)$ operations and sample $1^T\boldsymbol{N}(t_f)$ times from an inhomogeneous poisson process.



Uncontrolled, $\boldsymbol{N}(t_f)$ | CHESHIRE, $\boldsymbol{N}(t_f)$ | CHESHIRE, $\boldsymbol{M}(t_f)$ | Total number of actions

(a) Core-Periphery network



Uncontrolled, $\boldsymbol{N}(t_f)$ | CHESHIRE, $\boldsymbol{N}(t_f)$ | CHESHIRE, $\boldsymbol{M}(t_f)$ | Total number of actions

(b) Dissortative network

Figure 1: Activity on two 64-node networks, G_1 (top) and G_2 (bottom) under uncontrolled (Eq. 2; without CHESHIRE) and controlled (Eq. 4; with CHESHIRE) dynamics. The first and second columns visualize the final number of non incentivized actions $\boldsymbol{N}(t_f)$ under uncontrolled and controlled dynamics, where darker red corresponds to higher number of actions. The third column visualizes the final number of incentivized actions $\boldsymbol{M}(t_f)$ under controlled dynamics, where darker green corresponds to higher number of actions. The fourth column shows the temporal evolution of the number of incentivized and non incentivized actions across the whole networks for controlled and uncontrolled dynamics, where the solid line is the average across simulation runs and the shadowed region represents the standard error. By incentivizing a relatively small number of actions (∼3,600 actions), CHESHIRE is able to increase the overall number of (non incentivized) actions dramatically (∼96,000 vs ∼4,800 actions).

5 Experiments

5.1 Experiments on synthetic data

In this section, we shed light on CHESHIRE's sampling strategy in two small Kronecker networks [19] by recording, on the one hand, the number of incentivized actions per node and, on the other hand, the number of additional actions per node these incentivized actions triggers in comparison with an uncontrolled setup. Additionally, Appendix F compares the performance of our method against several baselines and state of the art methods [8, 10] on a variety of large synthetic networks and provides a scalability analysis.

Experimental setup. We experiment with two small Kronecker networks with 64 nodes, a small core-periphery (parameter matrix $[0.96, 0.3; 0.3, 0.96]$) and a dissortative network ($[0.3, 0.96; 0.96, 0.3]$), shown in Figure 1. For each network, we draw $\boldsymbol{A}$ from a uniform distribution $U(0, 10)$, $\boldsymbol{\mu}$ also from a uniform distribution $U(0, 10)$ for 20% of the nodes and $\boldsymbol{\mu} = 0$ for the remaining 80%, and set $\omega = 16$, $t_0 = 0$ and $t_f = 5.5$. Then, we compare the number of actions over time under uncontrolled dynamics (Eq. 2; without CHESHIRE) and controlled dynamics (Eq. 4; with CHESHIRE). In both cases, we perform 20 simulation

[2] In practice, we will consider diagonal matrices.

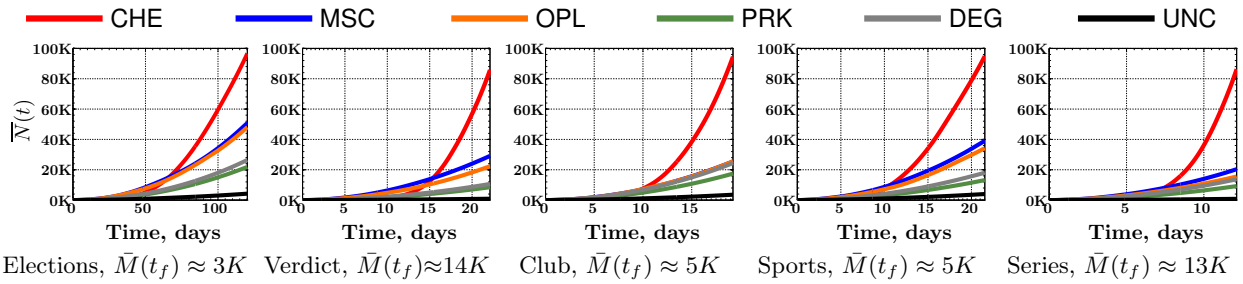


Figure 2: Performance over time of CHESHIRE against several competitors for each Twitter dataset. Performance is measured in terms of overall number of tweets $\bar{N}(t) = \sum_{u \in \mathcal{V}} \mathbb{E}[N_u(t)]$. In all cases, we tune the parameters $\boldsymbol{Q}$, $\boldsymbol{S}$ and $\boldsymbol{F}$ to be diagonal matrices such that the total number of incentivized tweets *posted* by our method is equal to the budget used in the competing methods and baselines. CHESHIRE (in red) consistently outperforms competing methods over time and it triggers up to 100%–400% more posts than the second best performer (in blue) as time goes by.

runs and sample (non incentivized) actions from a multidimensional Hawkes process using Ogata's thinning algorithm [23]. In the case of controlled dynamics, we sample incentivized actions using Algorithm 1.

Results. Figure 1 summarizes the results in terms of the number of non incentivized and incentivized actions, which show that: (i) a relatively small number of incentivized actions (fourth column; ∼3,600 actions) results in a dramatic increase in the overall number of (non incentivized) actions with respect the uncontrolled setup (fourth column; ∼96,000 vs ∼4,800 actions); (ii) the majority of the incentivized actions concentrate in a small set of influential nodes (third column; nodes in dark green); and, (iii) the variance of the overall number of actions (fourth column; shadowed regions) is consistently reduced when using CHESHIRE, in other words, the networks become more robust.

5.2 Experiments on real data

In this section, we experiment with data gathered from Twitter and show that our model can maximize the number of online actions more effectively than several baselines and state of the art methods [8, 10].

Experimental setup. We experiment with five Twitter datasets about current real-world events (Elections, Verdict, Club, Sports, TV Show), where actions are tweets (and retweets). Appendix G contains further details and statistics about these datasets. We compare the performance of our algorithm, CHESHIRE, with two state of the art methods, which we denote as OPL [8] and MSC [10], and two baselines, which we denote as PRK and DEG. PRK and DEG distribute the users' control intensities $\mathbf{u}(t)$ proportionally to the user's page rank and outgoing degree in the network, respectively. More in detail, we proceed as follows.

For each dataset, we estimate the influence matrix $\boldsymbol{A}$ of the multidimensional Hawkes process defined by Eq. 1 using maximum likelihood, as elsewhere [7, 29]. Moreover, we set the decay parameter ω of the corresponding exponential triggering kernel $\kappa(t)$ by cross-validation. Then, we perform 20 simulation runs for each method and baseline, where we sample non incentivized actions from the multidimensional Hawkes process learned from the corresponding Twitter dataset using Ogata's thinning algorithm [23]. For the competing methods and baselines, the control intensities $\boldsymbol{u}(t)$ are deterministic and thus we only need to sample incentivized actions from inhomogeneous poisson processes [21]. For our method, the control intensities are stochastic and thus we sample incentivized actions using Algorithm 1. Finally, we compare their performance in terms of the (empirical) average number of tweets $\mathbb{E}[\boldsymbol{N}(t)]$. In the above procedure, for a fair comparison, we tune the parameters $\boldsymbol{Q}$, $\boldsymbol{S}$ and $\boldsymbol{F}$ to be diagonal matrices such that the total number of incentivized tweets *posted* by our method is equal to the budget used in the state of the art methods and baselines.

Results. We first compare the performance of our algorithm against others in terms of overall average number of tweets $\bar{N}(t) = \sum_{u \in \mathcal{V}} \mathbb{E}[N_u(t)]$ for a fixed budget $\bar{M}(t_f) = \sum_{u \in \mathcal{V}} \mathbb{E}[M_u(t_f)]$. Figure 2 summarizes

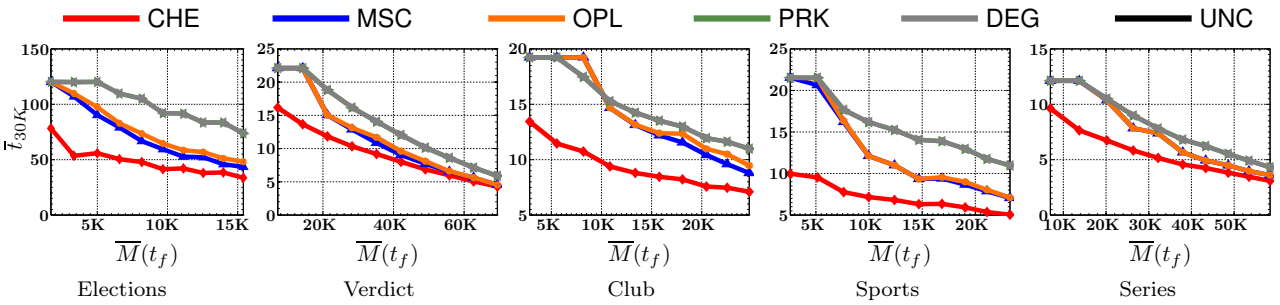


Figure 3: Performance vs. number of incentivized tweets for each Twitter dataset. Performance is measured in terms of the average time $\bar{t}_{30K}$ required by each method to reach a milestone of 30,000 tweets. CHESHIRE (in red) consistently reaches the milestone faster than the competing methods, *e.g.*, 20%–50% faster than the second best performer (in blue) for low budgets.

the results, which show that: (i) our algorithm consistently outperforms competing methods by large margins; (ii) it triggers up to 100%–400% more posts than the second best performer as time goes by; and, (iii) the baselines PRK and DEG have an underwhelming performance, suggesting that the network structure alone is not an accurate measure of influence.

Next, we evaluate the performance of our algorithm against others with respect to the available budget. To this aim, we compute the average time $\bar{t}_{30K}$ required by each method to reach a milestone of 30,000 tweets against the number of incentivized tweets $\bar{M}(t_f)$ (*i.e.*, the budget). Here, we do not report the results for the uncontrolled dynamics (UNC) since it did not reach the milestone after 10× the time the slowest competitor took to reach it. Figure 3 summarizes the results, which show that: (i) our algorithm consistently reaches the milestone faster than the competing methods; (ii) it exhibits a greater competitive advantage when the budget is low; and, (iii) it reaches the milestone 20%–50% faster than the second best performer for low budgets.

6 Conclusions

In this paper, we tackle the problem of activity maximization in social networks from the perspective of stochastic optimal control of temporal point processes and showed that the optimal level of incentivized actions depends linearly on the current level of overall actions. Moreover, the coefficients of this linear relationship can be found by solving a matrix Riccati differential equation, which can be solved efficiently, and a first order differential equation, which has a closed form solution. As a result, we were able to design CHESHIRE (Algorithm 1), an efficient and relatively simple online algorithm to sample the optimal times of the users' incentivized actions. We experimented with synthetic and real-world data gathered from Twitter and showed that our algorithm is able to consistently maximize activity more effectively than the state of the art.

Our work also opens many interesting venues for future work. For example, CHESHIRE optimizes a sum of quadratic losses on the users' intensities and assumes the influence matrix does not change over time, however, it would be useful to derive the optimal level of incentivized actions for other losses, *e.g.*, minimax loss, and consider time-varying influence. One of the challenges one would face is to find solutions that ensure the nonnegativity of the control intensity. Moreover, our experimental evaluation is based on simulation, using models whose parameters $(\boldsymbol{A}, \omega)$ are learned from data. It would be very interesting to evaluate our method using actual interventions in a social network. Finally, optimal control of jump SDEs with doubly stochastic temporal point processes can be potentially applied to design online algorithms for a wide variety of control problems in social and information systems, such as human learning [24], opinion control [30], and rumor control [11].

References

[1] O. Aalen, O. Borgan, and H. Gjessing. *Survival and event history analysis: a process point of view*. Springer Science & Business Media, 2008.

[2] D. Bertsekas. *Dynamic programming and optimal control*, volume 1. Athena Scientific Belmont, MA, 1995.

[3] L. Carroll. *Through the looking glass: And what Alice found there*. Rand, McNally, 1917.

[4] W. Chen, C. Wang, and Y. Wang. Scalable influence maximization for prevalent viral marketing in large-scale social networks. In *Proceedings of the 16th ACM SIGKDD international conference on Knowledge discovery and data mining*, pages 1029–1038. ACM, 2010.

[5] A. De, I. Valera, N. Ganguly, S. Bhattacharya, and M. Gomez-Rodriguez. Learning and forecasting opinion dynamics in social networks. In *Advances in Neural Information Processing Systems*, 2016.

[6] N. Du, L. Song, M. Gomez-Rodriguez, and H. Zha. Scalable influence estimation in continuous-time diffusion networks. In *Advances in Neural Information Processing Systems*, pages 3147–3155, 2013.

[7] M. Farajtabar, N. Du, M. Gomez-Rodriguez, I. Valera, H. Zha, and L. Song. Shaping social activity by incentivizing users. In *Advances in neural information processing systems*, pages 2474–2482, 2014.

[8] M. Farajtabar, M. Gomez-Rodriguez, N. Du, M. Zamani, H. Zha, and L. Song. Back to the past: Source identification in diffusion networks from partially observed cascades. In *Proceedings of the 18th International Conference on Artificial Intelligence and Statistics*, 2015.

[9] M. Farajtabar, Y. Wang, M. Gomez-Rodriguez, S. Li, H. Zha, and L. Song. COEVOLVE: A joint point process model for information diffusion and network co-evolution. *Advances in Neural Information Processing Systems*, 2015.

[10] M. Farajtabar, X. Ye, S. Harati, L. Song, and H. Zha. Multistage campaigning in social networks. In *Advances in Neural Information Processing Systems*, pages 4718–4726, 2016.

[11] A. Friggeri, L. A. Adamic, D. Eckles, and J. Cheng. Rumor cascades. In *ICWSM*, 2014.

[12] C. Garrett. *Numerical integration of matrix Riccati differential equations with solution singularities*. PhD thesis, The University of Texas at Arlington, May 2013.

[13] M. Gomez-Rodriguez, D. Balduzzi, and B. Schölkopf. Uncovering the temporal dynamics of diffusion networks. In *Proceedings of the 28th International Conference on Machine Learning (ICML'11)*, pages 561–568, 2011.

[14] F. Hanson. *Applied stochastic processes and control for Jump-diffusions: modeling, analysis, and computation*, volume 13. Siam, 2007.

[15] A. Hawkes. Spectra of some self-exciting and mutually exciting point processes. *Biometrika*, 58(1):83–90, 1971.

[16] M. Karimi, E. Tavakoli, M. Farajtabar, L. Song, and M. Gomez-Rodriguez. Smart Broadcasting: Do you want to be seen? In *Proceedings of the 22nd ACM SIGKDD International Conference on Knowledge Discovery in Data Mining*, 2016.

[17] D. Kempe, J. Kleinberg, and É. Tardos. Maximizing the spread of influence through a social network. In *Proceedings of the ninth ACM SIGKDD international conference on Knowledge discovery and data mining*, pages 137–146. ACM, 2003.

[18] J. Kingman. *Poisson processes*. Oxford university press, 1992.

[19] J. Leskovec, D. Chakrabarti, J. Kleinberg, C. Faloutsos, and Z. Ghahramani. Kronecker graphs: An approach to modeling networks. *The Journal of Machine Learning Research*, 11:985–1042, 2010.

[20] J. Leskovec, D. Chakrabarti, J. M. Kleinberg, C. Faloutsos, and Z. Ghahramani. Kronecker graphs: An approach to modeling networks. *JMLR*, 2010.

[21] P. A. Lewis and G. S. Shedler. Simulation of nonhomogeneous poisson processes by thinning. *Naval research logistics quarterly*, 26(3):403–413, 1979.

[22] C. Mavroforakis, I. Valera, and M. Gomez-Rodriguez. Modeling the dynamics of online learning activity. In *Proceedings of the 26th International World Wide Web Conference*, 2017.

[23] Y. Ogata. On lewis' simulation method for point processes. *Information Theory, IEEE Transactions on*, 27(1):23–31, 1981.

[24] S. Reddy, I. Labutov, S. Banerjee, and T. Joachims. Unbounded human learning: Optimal scheduling for spaced repetition. *Proceedings of the 22nd ACM SIGKDD International Conference on Knowledge Discovery and Data Mining*, 2016.

[25] M. Richardson and P. Domingos. Mining knowledge-sharing sites for viral marketing. In *Proceedings of the eighth ACM SIGKDD international conference on Knowledge discovery and data mining*, pages 61–70. ACM, 2002.

[26] N. Spasojevic, Z. Li, A. Rao, and P. Bhattacharyya. When-to-post on social networks. In *Proceedings of the 21th ACM SIGKDD International Conference on Knowledge Discovery and Data Mining*, pages 2127–2136. ACM, 2015.

[27] M. Stone. The generalized weierstrass approximation theorem. *Mathematics Magazine*, 21(5):237–254, 1948.

[28] B. Tabibian, I. Valera, M. Farajtabar, L. Song, B. Schoelkopf, and M. Gomez-Rodriguez. Distilling information reliability and source trustworthiness from digital traces. In *Proceedings of the 26th International World Wide Web Conference*, 2017.

[29] I. Valera, M. Gomez-Rodriguez, and K. Gummadi. Modeling diffusion of competing products and conventions in social media. *ICDM*, 2015.

[30] Y. Wang, E. Theodorou, A. Verma, and L. Song. A unifying framework for guiding point processes with stochastic intensity functions. *arXiv preprint arXiv:1701.08585*, 2017.

[31] A. Zarezade, U. Upadhyay, H. Rabiee, and M. Gomez-Rodriguez. Redqueen: An online algorithm for smart broadcasting in social networks. In *Proceedings of the 10th ACM International Conference on Web Search and Data Mining*, 2017.

[32] Q. Zhao, M. Erdogdu, H. He, A. Rajaraman, and J. Leskovec. Seismic: A self-exciting point process model for predicting tweet popularity. In *Proceedings of the 21th ACM SIGKDD International Conference on Knowledge Discovery and Data Mining*, 2015.

A Proof of Proposition 1

Using the left continuity of poisson processes and the definition of derivative $d\boldsymbol{\lambda}(t) = \boldsymbol{\lambda}(t+dt) - \boldsymbol{\lambda}(t)$ we can find the dynamics of the process by the Ito's calculus [14] as follows:

$$\begin{aligned}
d\boldsymbol{\lambda}(t) &= \boldsymbol{A}\int_0^{t+dt} g(t+dt-s)\,d\boldsymbol{N}(s) - \boldsymbol{A}\int_0^{t} g(t-s)\,d\boldsymbol{N}(s)\\
&= \boldsymbol{A}\int_0^{t+dt} (g(t-s)+g'(t-s)dt)\,d\boldsymbol{N}(s) - \boldsymbol{A}\int_0^{t} g(t-s)\,d\boldsymbol{N}(s)\\
&= \boldsymbol{A}\int_t^{t+dt} g(t-s)\,d\boldsymbol{N}(s) + dt\,\boldsymbol{A}\int_0^{t+dt} g'(t-s)\,d\boldsymbol{N}(s)\\
&= \boldsymbol{A}\,g(0)\,d\boldsymbol{N}(t) - w\,dt\,\boldsymbol{A}\int_0^{t+dt} g(t-s)\,d\boldsymbol{N}(s)\\
&= \boldsymbol{A}\,d\boldsymbol{N}(t) - w\,dt\,\boldsymbol{A}\int_0^{t} g(t-s)\,d\boldsymbol{N}(s)\\
&= \boldsymbol{A}\,d\boldsymbol{N}(t) + w\,dt\,[\boldsymbol{\mu}_0(t) - \boldsymbol{\lambda}(t)]
\end{aligned}$$

B Proof of Theorem 4

$$\begin{aligned}
&J(\boldsymbol{\lambda}(t),t) = \min_{\boldsymbol{u}(t,t_f]} \mathbb{E}_{(\boldsymbol{N},\boldsymbol{M})(t,t_f]}\left[\phi(\boldsymbol{\lambda}(t_f)) + \int_t^{t_f} \ell(\boldsymbol{\lambda}(s),\boldsymbol{u}(s))\,ds\right]\\
&= \min_{\boldsymbol{u}(t,t_f]} \mathbb{E}_{(\boldsymbol{N},\boldsymbol{M})(t,t_f]}\left[\phi(\boldsymbol{\lambda}(t_f)) + \int_t^{t+dt} \ell(\boldsymbol{\lambda}(s),\boldsymbol{u}(s))\,ds + \int_{t+dt}^{t_f} \ell(\boldsymbol{\lambda}(s),\boldsymbol{u}(s))\,ds\right]\\
&= \min_{\boldsymbol{u}(t,t_f]} \mathbb{E}_{(\boldsymbol{N},\boldsymbol{M})(t,t+dt]}\left[\mathbb{E}_{(\boldsymbol{N},\boldsymbol{M})(t+dt,t_f]}\left[\phi(\boldsymbol{\lambda}(t_f)) + \ell(\boldsymbol{\lambda}(t),\boldsymbol{u}(t))\,dt + \int_{t+dt}^{t_f} \ell(\boldsymbol{\lambda}(s),\boldsymbol{u}(s))\,ds\right]\right]\\
&= \min_{\boldsymbol{u}(t,t+dt]} \min_{\boldsymbol{u}(t+dt,t_f]} \mathbb{E}_{(\boldsymbol{N},\boldsymbol{M})(t,t+dt]}\left[\ell(\boldsymbol{\lambda}(t),\lambda(t),t)\,dt + \mathbb{E}_{(\boldsymbol{N},\boldsymbol{M})(t+dt,t_f]}\left[\phi(\boldsymbol{\lambda}(t_f)) + \int_{t+dt}^{t_f} \ell(\boldsymbol{\lambda}(s),\boldsymbol{u}(s))\,ds\right]\right]\\
&= \min_{\boldsymbol{u}(t,t+dt]} \mathbb{E}_{(\boldsymbol{N},\boldsymbol{M})(t,t+dt]}\left[J(\boldsymbol{\lambda}(t+dt),t+dt)\right] + \ell(\boldsymbol{\lambda}(t),\boldsymbol{u}(t))\,dt
\end{aligned}$$

C Proof of Theorem 5

Using the definition of derivative we can evaluate the differential of the cost-to-go as follows:

$$\begin{aligned}
dJ(\boldsymbol{\lambda}(t),t) &= J(\boldsymbol{\lambda}(t+dt),t+dt) - J(\boldsymbol{\lambda}(t),t)\\
&= J(\boldsymbol{\lambda}(t)+d\boldsymbol{\lambda}(t),t+dt) - J(\boldsymbol{\lambda}(t),t).
\end{aligned}$$

To evaluate the first term in the right hand side of the above equality we substitute $d\boldsymbol{\lambda}(t)$ by the SDE dynamics (4). Then, using the zero-one jump law [18] we can write:

$$
\begin{aligned}
&J(\boldsymbol{\lambda}(t) + d\boldsymbol{\lambda}(t), t + dt) = J(\boldsymbol{\lambda}(t) + f(t)\, dt + \boldsymbol{A}\, d\boldsymbol{N}(t) + \boldsymbol{A}\, d\boldsymbol{M}(t), t + dt) \\
&= \sum_i J(\boldsymbol{\lambda}(t) + f(t)\, dt + \boldsymbol{a}_i, t + dt) dN_i(t) + \sum_i J(\boldsymbol{\lambda}(t) + f(t)\, dt + \boldsymbol{a}_i, t + dt) dM_i(t) \\
&\quad + J(\boldsymbol{\lambda}(t) + f(t)\, dt, t + dt) \prod_i [1 - dN_i(t)][1 - dM_i(t)] \\
&= J(\boldsymbol{\lambda}(t) + f(t)\, dt, t + dt)[1 - \sum_i dN_i(t) + dM_i(t)] + \sum_i J(\boldsymbol{\lambda}(t) + f(t)\, dt + \boldsymbol{a}_i, t + dt)[dN_i(t) + dM_i(t)] \\
&= J(\boldsymbol{\lambda}(t) + f(t)\, dt, t + dt) + \sum_i [J(\boldsymbol{\lambda}(t) + f(t)\, dt + \boldsymbol{a}_i, t + dt) - J(\boldsymbol{\lambda}(t) + f(t)\, dt, t + dt)][dN_i(t) + dM_i(t)]
\end{aligned}
$$

where we denote $f(t) := w\boldsymbol{\mu}_0 - w\boldsymbol{\lambda}(t)$ for notation simplicity, and used that the bilinear differential form $dt\, dN(t) = 0$ as in [14]. By total derivative rule we have:

$$
\begin{aligned}
J(\boldsymbol{\lambda}(t) + f(t)\, dt + \boldsymbol{a}_i, t + dt) &= J(\boldsymbol{\lambda}(t) + \boldsymbol{a}_i, t) + \nabla_{\boldsymbol{\lambda}} J(\boldsymbol{\lambda}(t) + \boldsymbol{a}_i, t) f(t)\, dt + J_t(\boldsymbol{\lambda}(t) + \boldsymbol{a}_i, t)\, dt \\
J(\boldsymbol{\lambda}(t) + f(t)\, dt, t + dt) &= J(\boldsymbol{\lambda}(t), t) + \nabla_{\boldsymbol{\lambda}} J(\boldsymbol{\lambda}(t), t) f(t)\, dt + J_t(\boldsymbol{\lambda}(t), t)\, dt.
\end{aligned}
$$

If we plug these two relation in to the previous one, it results to:

$$
\begin{aligned}
J(\boldsymbol{\lambda}(t) + d\boldsymbol{\lambda}(t), t + dt) &= J(\boldsymbol{\lambda}(t), t) + \nabla_{\boldsymbol{\lambda}} J(\boldsymbol{\lambda}(t), t) f(t)\, dt + J_t(\boldsymbol{\lambda}(t), t)\, dt \\
&\quad + \sum_i [J(\boldsymbol{\lambda}(t) + \boldsymbol{a}_i, t) - J(\boldsymbol{\lambda}(t), t)][dN_i(t) + dM_i(t)],
\end{aligned}
$$

which completes the proof.

D Proof of $(\Delta_A J)_i \leq 0$

Lets $t < s$, then according to the definition we can write,

$$
\boldsymbol{\lambda}(s) = \boldsymbol{\mu}_0 + \int_0^s g(s - \tau)\, \boldsymbol{A}\, d\boldsymbol{N}(\tau) = \boldsymbol{\mu}_0 + \int_0^t g(s - \tau)\, \boldsymbol{A}\, d\boldsymbol{N}(\tau) + \int_t^s g(s - \tau)\, \boldsymbol{A}\, d\boldsymbol{N}(\tau).
$$

For the exponential kernel $g(t) = e^{-wt}$ we have,

$$
\int_0^t g(s - \tau)\, \boldsymbol{A}\, d\boldsymbol{N}(\tau) = \int_0^t e^{-w(s-\tau)}\, \boldsymbol{A}\, d\boldsymbol{N}(\tau) = e^{-w(s-t)} \int_0^t e^{-w(t-\tau)}\, \boldsymbol{A}\, d\boldsymbol{N}(\tau) = e^{-w(s-t)}(\boldsymbol{\lambda}(t) - \boldsymbol{\mu}_0)
$$

so given the value of $\boldsymbol{\lambda}(t)$ at time t then we can write $\boldsymbol{\lambda}(s)$ for later times as

$$
\boldsymbol{\lambda}(s) = \boldsymbol{\mu}_0 + e^{-w(s-t)}(\boldsymbol{\lambda}(t) - \boldsymbol{\mu}_0) + \int_t^s g(s - \tau)\, \boldsymbol{A}\, d\boldsymbol{N}(\tau)
$$

Lets consider a process $\boldsymbol{\xi}(s)$ with intensity value at time t equal to $\boldsymbol{\lambda}(t) + \boldsymbol{a}_i$ as,

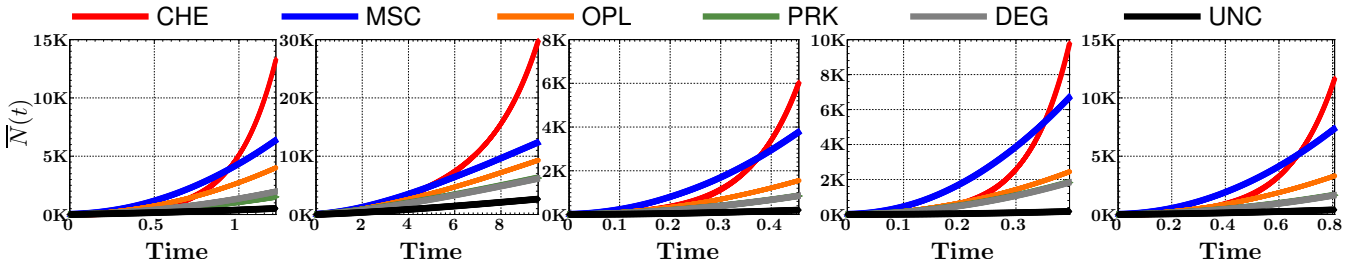
$$
\boldsymbol{\xi}(s) = \boldsymbol{\mu}_0 + e^{-w(s-t)}(\boldsymbol{\lambda}(t) + \boldsymbol{a}_i - \boldsymbol{\mu}_0) + \int_t^s g(s - \tau)\, \boldsymbol{A}\, d\boldsymbol{N}(\tau).
$$

Since $\boldsymbol{a}_i \succeq 0$, then given the same history in interval (t, s), we have $\boldsymbol{\xi}(s) \succeq \boldsymbol{\lambda}(s)$. Then, we have:

$$
\ell(\boldsymbol{\xi}(s), \boldsymbol{u}(s)) \leq \ell(\boldsymbol{\lambda}(s), \boldsymbol{u}(s)).
$$

Now, taking the integration, then expectation (over all histories) and finally the minimization from the above inequality does not change the direction of inequality. So it readily follows the required result.

$$
J(\boldsymbol{\lambda}(t) + \boldsymbol{a}_i, t) \leq J(\boldsymbol{\lambda}(t), t)
$$



(a) Core-periphery (b) Hierarchical (c) Homophily (d) Heterophily (e) Random

Figure 4: Performance over time of CHESHIRE against several competitors for several types of Kronecker networks. Performance is measured in terms of overall number of tweets $\bar{N}(t) = \sum_{u \in \mathcal{V}} \mathbb{E}[N_u(t)]$. In all cases, we tune the parameters Q, S and F such that the total number of incentivized tweets *posted* by our method is equal to the budget used in the competing methods and baselines.

E Proof of Lemma 6

Consider the following proposal of degree three for the cost-to-go function:

$$J(\boldsymbol{\lambda}(t), t) = f(t) + \sum_i g_i(t)\lambda_i(t) + \sum_i \sum_j \lambda_i(t)\lambda_j(t)H_{ij}(t) + \sum_i \sum_j \sum_k \lambda_i(t)\lambda_j(t)\lambda_k(t)H_{ijk}(t)$$

If we plug this proposal in Eq. 9, and evaluate the coefficient of fourth degree terms like $\lambda_i^2(t)\lambda_j^2(t)$ and equate them to zero, then we can find the unknown coefficients $H_{ijk}(t)$'s as follows:

$$\forall i, j, t : \sum_k \big(\sum_\ell A_{\ell k}^2\big) H_{ijk}^2(t) = 0$$

Since the sum of positives terms is zero if and only if they all be zero, then $H_{ijk}(t)$ and consequently the terms with degree three in the proposal are all zero. So the proposal reduces to a quadratic proposal.

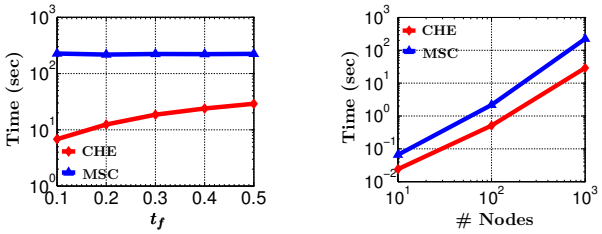
It is quite straightforward to extend this argument for proposals with order $m > 3$ and by equating the degree $2m - 1$ terms, similarly conclude that coefficients of degree m terms in the proposal are zero. If we repeat this argument for $m - 1, \ldots, 3$, we deduce that any proposal with arbitrary degree $m \geq 2$, would result in a quadratic optimal cost.

Finally, according to the Stone-Weierstrass theorem, any continuous function in a closed interval can be approximated as closely as desired by a polynomial function [27]. So by assuming the continuity of cost function, it can be approximate by a polynomial as closely as desired, and then it also reduce to a quadratic proposal too.

F Additional Experiments on Synthetic Data

Experimental setup. In this section, we experiment with five different types of Kronecker networks [20] with 512 nodes: (i) assortative networks (parameter matrix $[0.96, 0.3; 0.3, 0.96]$); (ii) dissortative networks ($[0.3, 0.96; 0.96, 0.3]$); (iii) random networks ($[0.7, 0.7; 0.7, 0.7]$); (iv) hierarchical networks ($[0.9, 0.1; 0.1, 0.9]$); and, (v) core-periphery networks ($[0.9, 0.5; 0.5, 0.3]$). For each network, we draw $\boldsymbol{\mu}$ and $\boldsymbol{A}$ from a uniform distribution $U(0, 1)$ and set $\omega = 100$. Similarly as in the experiments with Twitter data, we compare the performance of our algorithm with two state of the art methods, OPL [8] and MSC [10], and three baselines, PRK, DEG and UNC.

Performance. Figure 5 compares the performance of our algorithm against others in terms of overall average number of tweets $\bar{N}(t) = \sum_{u \in \mathcal{V}} \mathbb{E}[N_u(t)]$ for a fixed budget $\bar{M}(t_f) = \sum_{u \in \mathcal{V}} M_u(t_f) \approx 6.1$K. We find that: (i) our algorithm consistently outperforms competing methods by large margins at time t_f; (ii) it triggers up to 50%–100% more posts than the second best performer by time t_f; (iii) MSC tends to use the



(a) Running time vs t_f

(b) Running time vs #nodes

Figure 5: Scalability of CHESHIRE against several competitors. Panel (a) shows the running time against the cut-off time t_f for a 1,000 node Kronecker network. Panel (b) shows the running time for several Kronecker networks of increasing size with $t_f = 0.5$. In both panels, the average degree per node is 10. The experiments are carried out in a single machine with 24 cores and 64 GB of main memory.

budget too early, as a consequence, although it initially beats our method, it eventually gets outperformed by time t_f; and, (iv) the baselines PRK and DEG have an underwhelming performance, suggesting that the network structure alone is not an accurate measure of influence.

Scalability. Figure 5 shows that our algorithm scales to large networks and is almost an order of magnitude faster than the second best performer, MSC [10]. For example, our algorithm takes ∼30 seconds to steer a network with 1,000 nodes and average degree of 10 while MSC takes ∼4 minutes.

G Twitter Datasets Description

We used the Twitter search API[3] to collect all the tweets (corresponding to a 2-3 weeks period around the event date) that contain hashtags related to the following events/topics:

- **Elections:** British election, from May 7 to May 15, 2015.
- **Verdict:** Verdict for the corruption-case against Jayalalitha, an Indian politician, from May 6 to May 17, 2015.
- **Club:** Barcelona getting the first place in La-liga, from May 8 to May 16, 2016.
- **Sports:** Champions League final in 2015, between Juventus and Real Madrid, from May 8 to May 16, 2015.
- **TV Show:** The promotion on the TV show "Games of Thrones", from May 4 to May 12, 2015.

We then built the follower-followee network for the users that posted the collected tweets using the Twitter rest API[4]. Finally, we filtered out users that posted less than 200 tweets during the account lifetime, follow less than 100 users, or have less than 50 followers. An account of the dataset statistics is given in Table 1.

Dataset	$\lvert\mathcal{V}\rvert$	$\lvert\mathcal{E}\rvert$	$\lvert\mathcal{H}(T_{\mathbf{Data}})\rvert$	$T = T_{\mathbf{simulation}}$
Elections	231	1108	1584	120.2
Verdict	1059	10691	17452	22.11
Club	703	4154	9409	19.23
Sports	703	4154	7431	21.53
TV Show	947	10253	13203	12.11

Table 1: Real datasets statistics

[3] https://dev.twitter.com/rest/public/search
[4] https://dev.twitter.com/rest/public